Single-Doppler Velocity Retrievals and Their Applications

Ming Xue[12], Jidong Gao[1] and Steve Weygandt[1]

[1]Center for Analysis and Prediction of Storms
[2]School of Meteorology
University of Oklahoma, Norman, OK 73019, USA

1. INTRODUCTION

Doppler radar has long been a valuable observational tool in meteorology. It has the capability of observing, at high spatial and temporal resolution, the internal structure of convective storm systems from remote locations. However, the direct measurements are limited to reflectivity and the radial component of velocity; there is no direct measurement of the complete three-dimensional (3D) wind field. To initialize storm-resolving numerical models, it is desirable to know the full wind field. Techniques for retrieving 3D wind fields given single-Doppler observations of radial velocity and reflectivity have been developed in recent years, many at the Center for Analysis and Prediction of Storms (CAPS), University of Oklahoma. To overcome the under-determinedness of the problem, almost all methods make use of data at multiple time levels and they are usually based on certain assumptions. A review of some of these methods can be found in Shapiro (1995a).

Qiu and Xu (1992) developed a so-called simple adjoint (SA) method that uses the observed reflectivity (or/and radial wind) as a quasi-conservative tracer. Using a variational procedure in which a conservation equation (with source terms) for the tracer and its adjoint are integrated over a period of successive radar scans, the time-mean wind field is retrieved. As a variational procedure, the SA method also permits the combined use of other physical constraints such as the mass continuity. Other observations and background information can be easily incorporated. Furthermore, the method does not have the boundary condition problems typical of most other methods.

The original SA method had been tested with remarkable success on simulated data and low-level boundary layer observations. It is, however, only designed to work in 2-D horizontal planes and the 3D mass continuity equation is not necessarily satisfied. The method may not work well for observations at high elevation angles, either. To avoid these shortcomings, the method is extended to a 3D formulation in the current work. As such, all three wind components are retrieved in a dynamically consistent manner using the entire volume of data set. The 3D instead of 2D mass-continuity equation can now be used directly, as a weak constraint in our case. The following section briefly describes the procedure then presents some testing results with simulated data. In Section 4, we will present a sample result from a recent realtime storm-scale numerical prediction experiment in which retrieved Doppler radar data are used in the initial condition.

Corresponding Author Address: Dr. Ming Xue, School of Meteorology, Sarkeys Energy Center, 100 East Boyd, Norman, OK 7319. E-mail: mxue@ou.edu

2. DESCRIPTION OF METHODOLOGY

a) Variational problem

The new SA method described herein retrieves the 3-D time-mean (over the retrieval period) wind-vector field (u_m, v_m, w_m) from single-Doppler observations of radial velocity (V_r^{ob}) and/or reflectivity (η^{ob}) spanning the retrieval period. A cost-function is defined as follows:

$$J = J_\eta + J_{V_{rm}} + J_B + J_D + J_S, \tag{1}$$

where the first term,

$$J_\eta = \frac{1}{2}\sum_{ijkn} W_\eta (\eta - \eta^{ob})^2, \tag{2}$$

defines the distance between predicted (η) and observed (η^{ob}) tracer (either reflectivity or radial wind). The summation is over all grid point (i, j, k) indices and time levels (n). η is "predicted" by a simplified 3D conservation (advection) equation:

$$\frac{\partial \eta}{\partial t} + u_m \frac{\partial \eta}{\partial x} + v_m \frac{\partial \eta}{\partial y} + w_m \frac{\partial \eta}{\partial z} - k_h \nabla_h^2 \eta - k_v \nabla_v^2 \eta = F_m \tag{3}$$

with the conditions of $\eta(t,x,y,z) = \eta^{ob}(t,x,y,z)$ at the domain boundary and $\eta(0,x,y,z) = \eta^{ob}(0,x,y,z)$ at the initial time. Here the superscript *ob* denotes observed values. The coefficient of eddy viscosity k_H and k_V are unknown constants to be retrieved. F_m is a source term that includes all other non-conservative effects, and it is also to be retrieved.

The second term in (1), $J_{V_{rm}}$, defines the distance between the analyzed (V_{rm}) and mean observed radial wind (V_{rm}^{ob}):

$$J_{V_{rm}} = 1/2 \sum_{ijk} W_{rm} (V_{rm} - V_{rm}^{ob})^2. \tag{4}$$

Here, V_{rm}^{ob} is obtained by averaging V_r^{ob} over the retrieval time period, and V_{rm} has the following relationship with u_m, v_m, w_m:

$$V_{rm} = (x u_m + y v_m + z w_m)/r \tag{5}$$

where r is radial distance from the radar.

The other terms in the cost function have the following definitions:

$$J_B = 1/2 \left[\sum_{ijk} W_{ub}(u_m - u_b)^2 + \sum_{ijk} W_{vb}(v_m - v_b)^2 + \sum_{ijk} W_{wb}(w_m - w_b)^2 \right], \tag{6}$$

$$J_D = 1/2 \sum_{ijk} W_D D^2, \tag{7}$$

$$J_S = 1/2 \left[\sum_{ijk} \lambda_{us} (\nabla^2 u)^2 + \sum_{ijk} \lambda_{vs} (\nabla^2 v)^2 + \sum_{ijk} \lambda_{ws} (\nabla^2 w)^2 \right]. \tag{8}$$

Here J_B measures how close the variational analysis is to the background field, and J_D imposes a weak anelastic mass continuity constraint on the analyzed wind field, where

$$D \equiv \frac{\partial \bar{\rho} u}{\partial x} + \frac{\partial \bar{\rho} v}{\partial y} + \frac{\partial \bar{\rho} w}{\partial z}, \tag{9}$$

and $\bar{\rho}$ is the mean air density profile.

The last term in the cost function, J_s, is a smoothness constraint.

In the above expressions, The *W's* are weighting coefficients that depend on the strength of the constraint and are chosen based on either experiences or statistics of observations. For our purpose, these coefficients are chosen according to the relative importance of each term.

To solve the above variational problem by direct minimization, we need to derive the gradient of the cost function with respect to the control variables (u_m, v_m, w_m, F_m, k_H, k_v). The gradient of J with respect to each variable is obtained by taking the variation of J with respect to each variable. Their actual formulations are omitted here.

In the gradient formulations for all of the gradients, a variable, η^*, appears which is the solution of the associated adjoint equation:

$$-\partial\eta^*/\partial t - \partial(u_m\eta^*)/\partial x - \partial(v_m\eta^*)/\partial y - \partial(w_m\eta^*)/\partial z - k_h\nabla_H^2\eta^* - k_v\nabla_v^2\eta^* = W_\eta(\eta - \eta^{ob}). \tag{10}$$

The boundary and initial values of (10) are given by $\eta*(t,x,y,z)=0$ at the domain boundary and $\eta*(T,x,y,z)=0$ at the ending time, T, of the retrieval period.

b) Solution Procedure

After the gradients of cost function are obtained, the problem can be solved with the following procedure:

(1) Choose the first guess of control variable Z=(u_m, v_m, w_m, F_m, k_H, k_v), integrate Eq.(3) from 0 to T and store the computed field;
(2) Calculate J using fields obtained from step (1);
(3) Integrate adjoint equation (10) from T to 0 and calculate the gradient of J with respect to each of the control variables;
(4) Obtain updated values of the control variable using a conjugate gradient method or a quasi Newton method (Navon, 1987)
(5) Check if the optimal solution has been found by computing the norm of the gradients or the value of J to see if it is less than a prescribed tolerance. If yes, stop the iteration and output the optimal u_m, v_m, w_m, F_m, k_H, k_v where u_m, v_m, w_m are the desired velocity components to be retrieved.
(6) If the convergence criterion is not satisfied, steps 2 through 5 are repeated using updated values of Z as the new guess until convergence is reached.

Finally we point out that the observations of radial velocity are adjusted to remove the contribution of fall speed of precipitation particles.

3. TESTS WITH SIMULATED DATA

a) Experimental design

To evaluate the performance of our SA method, we utilize a set of simulated single-Doppler radar data. A well-documented tornadic supercell storm (Ray et al 1981) that occurred near Del City, Oklahoma on 20 May 1977 is used for the numerical experiments.

The Advanced Regional Prediction System (ARPS, Xue et al. 1995) developed at CAPS is used here to perform a two-hour simulation of this storm. The simulation starts from a thermal bubble placed in a horizontally homogeneous base state specified from the sounding used in Klemp et al. (1981). The model grid is comprised of 67x67x35 grid points and the grid interval is 1 km in the horizontal and 0.5 km in the vertical. The physical domain size is 64x64x16 km^3. Kessler-type warm rain microphysics is used together with 1.5-order TKE-based sub-grid turbulence parameterization and open conditions at the lateral boundaries.

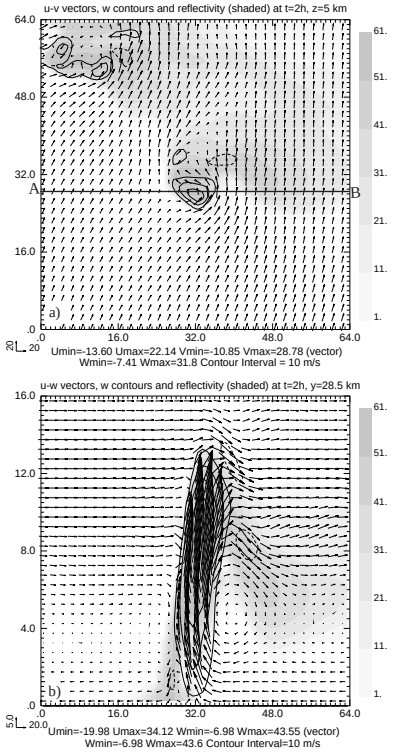

Figure 1. The ARPS model simulated wind vectors, vertical velocity w (contours) and simulated reflectivity (shaded) fields of the 20 May 1977 supercell storm at 2 hours. a) Horizontal cross-section at z = 5 km; b) Vertical cross-section through line A-B in a).

Figure 1 shows horizontal and vertical cross-sections of wind, vertical velocity (vertical cross-section is plotted through line A-B in Fig.1a), and reflectivity fields at two hours of the simulation. A strong rotating updraft and associated low-level downdraft are evident near the center of the domain while disturbances associated with the left mover from the earlier storm splitting are also clear. Downstream of the over-shooting updraft at the tropopause level are downward returning flows that exhibit gravitational oscillations

(Fig.1b). By this time, the simulated storm has attained a structure typically of mature supercell storms.

The simulated 3-D convective-scale wind field at two hours is sampled by single pseudo-radar, the radar is located at the NE corner of Fig 1a and at the ground level. The radial wind components are synthesized to obtain radial velocities at each model grid point according to Eq.(5). The simulated radial velocity at 7050s and 7350s are used as tracer observation.

To measure the accuracy of retrievals, the RMS and relative RMS errors as well as the correlation coefficients between the retrieval and the reference are calculated, for the horizontal and vertical velocities respectively.

b) Results of retrievals

Limited by space, we present here only results from the control experiment. In this experiment, all constraints discussed earlier were included and the first guesses for all the wind components and the forcing term in Eq.(3) were set to zero. k_h and k_v were set to 200 ms^{-2}. The retrieval results are presented in Fig 2. Comparing with Fig. 1, all important features in the horizontal wind field, including the curvature around and the convergence near the rotating updraft, are well retrieved (Fig 2a). In Fig. 2b, the general structure of the updraft is well retrieved at all levels and the downdraft in the western part of domain is also present. Oscillations downstream of the updraft top due to gravity waves are also evident.

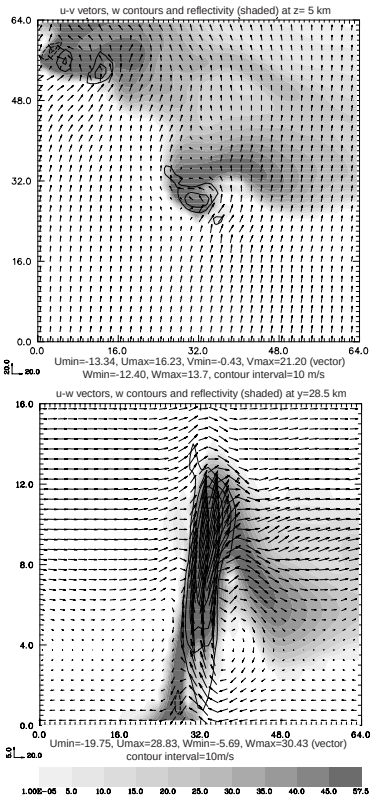

Figure 2. The wind vectors, the contours of vertical velocity difference between the retrieved wind and the referenced one. Others are same as Fig 1.

The relative RMS error is small (0.205) for horizontal wind. The RMS error for vertical velocity is larger (0.742) but the correlation coefficient is also reasonably large (0.691). This is so because most of the error is in the amplitude while the phase error is relatively small. The retrieved vertical velocity is considerably weaker than the true one.

The variation of the cost function and the norm of gradient for each constraint with respect to the number of iterations reveals that the background constraint accounts for the largest portion in the total cost function, the other constraints, including the simple conservation equation, mean radial velocity, and mass continuity constraints have about the same order of magnitude contributions to the total cost function. This indicates that the distance between the retrieval and the background (only given by a single sounding) remains large therefore the background constraint does not dominate the analysis field. The cost functions for the other constraints are reduced by more than four orders of magnitude at the end of 350 iterations.

In summary, satisfactory results have been obtained with simulated data using the newly developed 3D version of the simple-adjoint single-Doppler velocity retrieval method. Recently, good results using observed WSR-88D radar data have also been obtained and will be reported elsewhere. In the following, we will present a realtime forecast example that shows the impact of retrieved radar data.

4. AN EXAMPLE PREDICTION USING FULL RADAR RETRIEVAL

From mid-April through early June, 1999, CAPS conducted its most ambitious special operational forecasting experiment to date. Specifically, running on a 256-processor SGI Origin 2000 in distributed-memory mode, CAPS produced, on a daily basis, 5 ensembles at 32-km resolution, two 32-km resolution continental US forecasts, two regional forecasts at 9 km resolution, and up to three local forecasts at 3 km resolution. The higher resolution grids were nested one-way within the outer domains, and the boundary conditions for the outer-most grid were provided by the NCEP Eta model. For the first time ever, the forecasts used real time full-volume (Level-II) data from several WSR-88D radars. The overall retrieval procedure is outlined in Shapiro et al (1995a) and Weygandt et al (1998).

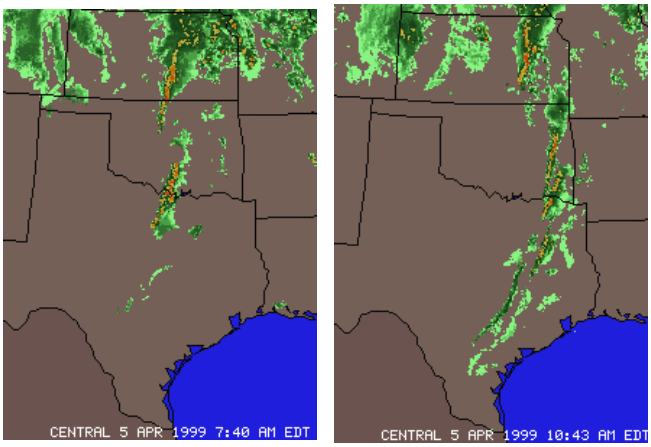

Figure 3. Radar reflectivity valid at approximately a) 12 UTC and b) 15 UTC on 5 April 1999.

The ARPS model performed very well during the period. We present here only one example that illustrates the benefits of WSR-88D data via retrievals. Figure 3. shows the composite reflectivity valid at 12 and 15 UTC on 5 April 1999. At 12 UTC, a strong storm system moving through the US Central Plains has triggered a segmented line of storms extending through central Kansas, southern Oklahoma and north-central Texas. By 15 UTC, the line has progressed eastward while the convection has maintained its intensity.

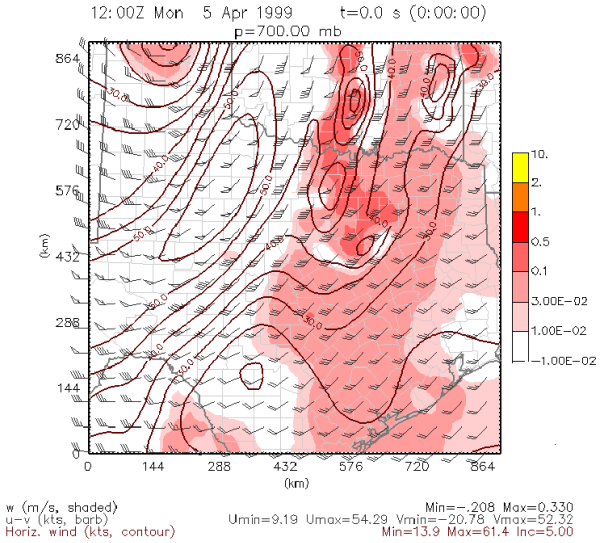

Figure 4. ARPS model initial condition, valid at 12 UTC April 5, 1999, of 700 mb vertical velocity (only shaded contours for positive w are shown in m/s), wind barbs, and isotachs (contours, kts) using Level II data with single Doppler velocity and thermodynamic retrievals.

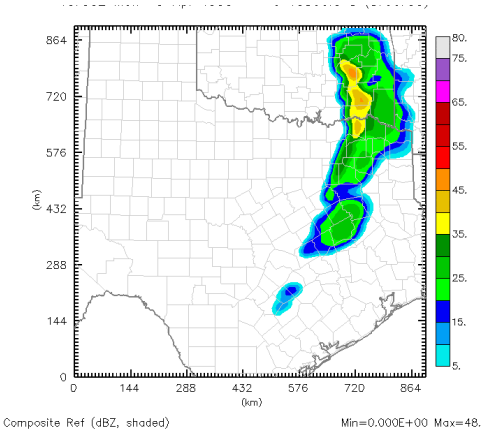

Figure 5. ARPS 3-hour, 9 km resolution forecast of composite reflectivity (dBz) valid 15 UTC on 5 April 1999, starting from the initial condition in Fig.4.

Figure 4 shows the 700 mb ARPS initial condition fields of vertical velocity, wind barbs, and isotachs using Level II data with single-Doppler velocity retrieval (Shapiro et al 1995a) and thermodynamic retrievals (Gal-Chen 1978). The retrievals provide a strong velocity signal which, when used as initial conditions in a 3 hour ARPS forecast at 9 km resolution, is able to capture the strong convection in southeastern Oklahoma that stretches into central Texas (Fig.4). The forecast without radar missed most of the convection (not shown). This is encouraging considering that significant smoothing occurred when the retrieved information is analyzed onto the 9-km grid through an analysis procedure in the ARPS Data Analysis System. Fuller impact is expected on grids with much higher resolutions. This, in fact, has been shown to be true for other cases. Currently, significant efforts are underway at CAPS to develop a 3DVAR procedure in which the retrieval from radar data and the analysis of other data are performed in a single variational framework and on the model native grid. The procedure is envisioned also to be used by the next generation US Weather Research and prediction model, the WRF.

Acknowledgments

This research was supported by NSF Grant ATM91-20009 to CAPS. Many scientists at CAPS contributed to the operational forecasting experiment.

Reference

Gal-Chen, T., 1978: A method for initializing the anlastic equations: Implications for matching models with observations. *Mon. Wea. Rev.,* **106**, 587-606.

Klemp, J. B., and R. B. Wilhelmson and P. S. Ray, 1981: Observed and numerically simulated structure of a mature supercell thunderstorm. *J. Atmos. Sci.*, **38**, 1558-1580.

Navon, I. M., and D. M. Legler, 1987: Conjugate-gradient methods for large-scale minimization in meteorology. *Mon. Wea. Rev.*, **115,** 1479-1502.

Qiu, C.-J., and Q. Xu, 1992: A simple adjoint method of wind analysis for single-Doppler data. *J. Atmos. And Oceanic Technol.*, **9**, 588-598**.**

Ray, P. S., B. C. Johnson, K. W. Johnson, J. S. Bradberry, J. J. Stephens, K. K. Wagner, R. B. Wilhelmson, and J. B. Klemp, 1981: The morphology of several tornadic storms on 20 May, 1977. *J. Atmos. Sci.*, **38**, 1643-1663.

Sasaki, Y., 1970: Some basic formalisms in numerical variational analysis. *Mon. Wea. Rev.*, **98**, 875-883.

Shapiro, A., S. Ellis, and J. Shaw,, 1995a: Single-Doppler velocity retrievals with Phoenix II data: clear air and microburst retrievals in the planetary boundary layer. *J. Atmos. Sci.*, **52**, 1265-1287.

Shapiro, A., K. Droegemeier, S. Lazarus, and S. Weygandt, 1995b: Forward variational four-dimensional data assimilation and prediction experiments using a storm-scale numerical model. *Int. Symp. Assimilation of Observations in Meteorology and Oceanography.* Tokyo, WMO, 361-366.

Weygandt, S. , A. Shapiro, and K. Droegemeier, 1998: The use of wind and thermodynamic retrievals to create initial forecast fields from single-Doppler observations of a supercell thunderstorm. Preprints, *11th Conf. on Wea Anal. and For.,* Phoenix, AZ, Amer. Meteor. Soc., 286-288.

Xue, M., K. K. Droegemeier, Vince Wong, A. Shapiro, and K. Brewster, 1995: Advanced Regional Prediction System (ARPS) Version 4.0 User's Guide, 380 pp. [Available from Center for Analysis and Prediction of Storms, University of Oklahoma, 100E. Boyd, Norman, OK 73019].